RESEARCH ARTICLE

JBMR®

Rapid Cortical Bone Loss at the Distal Radius Is Associated With Higher Risk of Fracture in Older Men – The STRAMBO Study

Elina Gunsing,[1] Philippe P. Wagner,[1] Danielle E. Whittier,[2] Steven K. Boyd,[2] Roland Chapurlat,[1] and Pawel Szulc[1]

[1]INSERM UMR 1033, University of Lyon, Hôpital Edouard Herriot, Lyon, France
[2]McCaig Institute for Bone and Joint Health, Department of Radiology, Cumming School of Medicine, University of Calgary, Calgary, Alberta, Canada

ABSTRACT

Rapid loss of areal bone mineral density (aBMD) is associated with higher fracture risk after adjustment for confounders including initial aBMD. However, the link between bone microarchitecture decline and fracture is not clear. We studied the association between bone microarchitecture deterioration assessed prospectively over 4 years and the subsequent fracture risk in older men. Bone microarchitecture at the distal radius and tibia was assessed by high-resolution peripheral QCT (HR-pQCT; XtremeCT, Scanco Medical) (baseline, 4 years) in 732 men aged 60–87 years. During the 8-year follow-up, 109 men had fragility fractures. Areal BMD was assessed by dual-energy X-ray absorptiometry. After adjustment for age, weight, prior falls and fractures, distal radius aBMD (baseline, slope), and baseline distal radius total volumetric BMD (Tt.BMD), a faster decrease in distal radius Tt.BMD was associated with higher fracture risk (hazard ratio [HR] = 1.54/SD, 95% confidence interval: 1.20–1.95, $p < .005$). Rapid cortical bone loss was associated with higher fracture risk (cortical thickness: HR = 1.48; 1.15–1.90, $p < .01$; cortical BMD: HR = 1.38; 1.11–1.72, $p < .01$). The rate of trabecular bone loss at the distal radius and the rate of bone microarchitecture decline at the distal tibia were not associated with fracture risk. After adjustment for aBMD and distal radius HR-pQCT measures assessed after 4 years, changes in Tt.BMD were associated with higher fracture risk (e.g., Tt.BMD: HR = 1.37; 1.11–1.69, $p < .005$). Compared with the reference model (age, weight, prior fractures and falls, baseline and slope of aBMD, baseline HR-pQCT value), further addition of the slope of the HR-pQCT measure did not improve the fracture prediction. Thus, rapid cortical bone loss at the distal radius is associated with higher fracture risk in the multivariable models including baseline values of the HR-pQCT measure. However, repeated HR-pQCT measurements did not improve the assessment of the fracture risk in older men (compared with the reference model defined earlier). © 2023 American Society for Bone and Mineral Research (ASBMR).

KEY WORDS: osteoporosis; HR-pQCT; fracture risk assessment; aging; DXA

Introduction

Osteoporosis is characterized by low bone mass and deterioration of microarchitecture, which result in a higher risk of fracture.[1] The main tool in fracture risk assessment is areal bone mineral density (aBMD) measured by dual energy X-ray absorptiometry (DXA) at the hip. Low aBMD is associated with a higher risk of fracture in men and women.[2,3]

Biomechanical studies show that bone microarchitecture is a major determinant of fracture risk.[4] In prospective studies, poor bone microarchitecture measured by high-resolution peripheral quantitative computed tomography (HR-pQCT) and low bone strength estimated by micro-finite element (μFE) analysis are associated with higher fracture risk after adjustment for potential confounders, including aBMD.[5-8] These patterns were found in older men and in postmenopausal women regardless of fracture type (fragility fracture, major osteoporotic fracture, spine fracture, nonspine fracture).

Areal BMD decreases with age, but the rate of bone loss (i.e., prospectively assessed decrease in aBMD) varies substantially across the population. Most studies have shown that rapid bone loss is associated with higher fracture risk after adjustment for confounders, including baseline aBMD.[9-25] However, patterns were inconsistent in early and late postmenopausal women as well as

Received in original form October 19, 2022; revised form March 10, 2023; accepted March 25, 2023.
Address correspondence to: Pawel Szulc, MD, PhD, INSERM UMR 1033, Hôpital Edouard Herriot, University of Lyon, Pavillon F, Place d'Arsonval, 69437 Lyon, France.
E-mail: pawel.szulc@inserm.fr
Additional Supporting Information may be found in the online version of this article.
Journal of Bone and Mineral Research, Vol. 38, No. 6, June 2023, pp 841–850.

DOI: 10.1002/jbmr.4811

in older men, and for different types of fracture (e.g., hip, spine, fragility fracture). The results did not depend on the definition of accelerated bone loss (i.e., continuous versus groups). The patterns were somewhat inconsistent for bone loss assessed at various skeletal sites (hip, distal forearm, ultradistal radius, lumbar spine). However, in older men, low aBMD at baseline, combined with high subsequent loss of aBMD, was associated with the highest risk of fracture, in particular hip fracture.[9]

The inconsistent results could be partly due to poor statistical power, method of measuring aBMD and skeletal site, inaccurate estimation of bone loss during a short interval, competing risk of death, or other factors. The repeated measures of aBMD do not improve the identification of older women or men at high risk of fragility fracture.[13-17,22] Men with rapid bone loss typically have poorer microarchitecture, thinner cortices, and lower estimated bone strength than men without rapid bone loss.[26] However, the link between the prospectively assessed decline in bone microarchitecture and fracture risk has not been thoroughly studied.

Therefore, our aim was to assess the association between the prospectively assessed decline in bone microarchitecture and the subsequent risk of fracture in a cohort of older men followed for 12 years.

Subjects and Methods

Cohort

The STRAMBO study is a single-center prospective cohort study of the skeletal fragility and its determinants in men.[27] It was carried out as a collaboration between the National Institute of Health and Medical Research (INSERM) and Mutuelle des Travailleurs de la Région Lyonnaise (MTRL). MTRL is a complementary health insurance company, open to all citizens. Insured individuals are representative of the French population in terms of age and socioeconomic status. The study obtained permission from the ethics committee and was performed according to the Helsinki Declaration (1975, 1983). Participants were recruited between 2006 and 2008 from the MTRL lists in Lyon. Letters inviting participation were sent to a randomly selected sample of men aged 20–85 years living in the greater Lyon area. Informed consent was provided by 1169 men. Men who were able to give informed consent, answer questionnaires, and participate in the diagnostic tests were included. No specific exclusion criteria were used. Men aged 60 and older ($n = 825$) were followed prospectively for 12 years and responded annually to a short questionnaire concerning incident nonspine fractures. After 4, 8, and 12 years, men had a full follow-up visit including DXA and high-resolution peripheral quantitative computed tomography (HR-pQCT) imaging. Transport to and from study visits was offered to enable men with reduced mobility to continue participation.

HR-pQCT

Bone microarchitecture was assessed at the nondominant distal radius and right distal tibia at baseline and 4 years using HR-pQCT (XtremeCT; Scanco Medical, Brüttisellen, Switzerland). The limb was fixed in a carbon-fiber shell to limit motion.[27] A reference line was placed at a fixed offset of 9.5 and 22.5 mm proximal to the endplate of the radius and tibia. A three-dimensional (3D) stack of 110 slices was acquired from the reference line, with an isotropic voxel size of 82 μm. The volume of interest (VOI) was separated into trabecular and cortical compartments using the standard threshold-based protocol.[28] Cortical thickness ($Ct.Th^d$, mm) was defined as the mean cortical volume divided by bone perimeter. Cortical and trabecular density (Ct.BMD, Tb.BMD, mg HA/cm^3) were calculated as average volumetric BMD (vBMD) within each compartment. Trabecular area (Tb.Ar) is progressively peeled by one pixel on the contour, and the remaining area is measured.[29] When it is <60% of the initial area, the process is stopped. The remaining area in the center is defined as the inner area, and the peeled area is defined as the subendocortical area. The densities in each area are called subendocortical and inner densities (s.e.Tb.BMD and inn.Tb.BMD, respectively). Trabecular elements were identified by mid-axis transformation method. Trabecular number (Tb.N, 1/mm) was assessed as the mean inverse of the spacing between trabecular mid-axes. Trabecular thickness ($Tb.Th^d$, μm) and separation ($Tb.Sp^d$, μm) were derived from the (bone volume)/(total volume) ratio and Tb.N. The intra-individual scatter of $Tb.Sp^d$ (Tb.1/N.SD, mm) reflects trabecular network heterogeneity. It is quantified as standard deviation (SD) of the distances between the mid-axes. Quality control was performed by daily scans of a phantom containing hydroxyapatite (HA) rods (densities of 0–800 mgHA/cm^3) embedded in a soft-tissue-equivalent resin (QRM, Moehrendorf, Germany). The coefficient of variation (CV) for the densities was 0.1%–0.9%.[29] In vivo CVs varied from 0.7% for Ct. BMD to 4.4% for $Tb.Th^d$.[29] The least significant change (LSC) for HR-pQCT measures varied from 2.0% to 12.1%. Registration of longitudinal measurements was performed based on the manufacturer's slice-based matching method. The scans with >70% of the overlap were retained. Separation of the cortical and trabecular compartments was performed automatically, and contours were checked visually and corrected as required.[30] At each visit, scans of poor quality (motion grade >3 on a scale from 1 to 5) were excluded.[31]

Finite-element analysis

Micro–finite-element (μFE) analysis was performed using unregistered segmented HR-pQCT images to estimate reaction force and failure load. Linear μFE models were generated using the voxel-by-voxel approach. A Poisson's ratio of 0.3 and a homogeneous Young's modulus of 6829 GPa were assigned as bone tissue properties.[32] The model boundary conditions were an axial compression test with 1% compressive strain, and resultant reaction force of the bone was measured. Failure load was estimated from the models using a yield criterion of 2% critical volume and 0.7% critical strain.[33] μFE models were solved using a conjugate gradient approach with a convergence criterion of 1×10^{-6} (FAIM version 8.0, Numerics88 Solutions Ltd, Canada) at the University of Calgary's High-Performance Computing cluster.

Incident fractures

We retained self-reported low-trauma nonspine fractures (fall from a standing position or less) confirmed by a health professional (X-ray, medical report). Lateral single-energy scans of the thoracic and lumbar spine (T4–L4) were obtained in the dorsal decubitus position using a Hologic Discovery-A (Hologic, Bedford, MA, USA) device equipped with rotating C-arm.[27] Scans were performed in all men at baseline and in those who returned for the follow-up visits (4, 8, and 12 years). Incident vertebral fractures were assessed on the follow-up scans.[5] A new incident fracture was diagnosed based on the visual analysis (endplate

fracture) and/or a decrease in any of the vertebral heights by >15% versus the previous scan. The vertebrae that were not clearly visible were considered nonfractured. Among 732 men who had a second HR-pQCT scan, 109 had incident fragility fractures (nonspine low-trauma fractures, spine fractures) after this scan (57 spine fractures in 49 men, rib 21, humerus 8, radius 9, pelvis 6, hip 16, femur 1, patella 2, ankle 6). In addition, six men had fractures of the face (one), metacarpal (one), index (one), big toe (one), and fractures related to high trauma (rib one, radius one). Thus, jointly, 115 men had fractures after 4 years.

Epidemiologic questionnaire

The men responded to an interviewer-administered questionnaire. They self-reported falls with no external force in the year prior to recruitment. Prior nonspine fractures self-reported at baseline were dichotomized (yes/no) and not further ascertained.[27] The fractures retained were low trauma fractures, except those of the skull, face, hand, fingers, and toes. Fractures related to high trauma were excluded. Prevalent spine fractures were assessed using a semiquantitative score on the baseline lateral DXA scans. Grade 2 and 3 fractures unrelated to a self-reported major trauma were retained.[34] Weight and height were measured using standard equipment.

Measurement methods

A DXA device (Hologic Discovery A, Hologic, Bedford, MA, USA) equipped with a rotating C-arm was used to measure baseline aBMD at the following regions of interest (ROIs): femoral neck, total hip, distal radius, ultradistal radius.[27]

Statistical methods

Statistical analyses were carried out using R software (version 1.4.1103). Data are presented as mean ± SD or as median and interquartile range (IQR). The shape of distribution was verified by histograms and quantile plots of the residuals. The selection of variables was based on the previously published data on fracture prediction by aBMD and bone microarchitectural measures. Fracture-free survival as a function of the HR-pQCT variables was analyzed by a Kaplan–Meier survival model, the Cox model, after verification of the proportional hazards hypothesis using Schoenfeld's residuals. The length of follow-up was censored at first fracture, death, last news, or end-of-study follow-up. The standardized variables were used to facilitate the comparison of the point estimates of the investigated associations. The models were adjusted progressively for age, weight, prior falls, prior fractures, baseline value of HR-pQCT measure (investigated in the given model), and baseline value and 4-year loss of aBMD (ultradistal or middistal radius for the analysis of the distal radius HR-pQCT indices and femoral neck or total hip for the analysis of the distal tibia HR-pQCT indices). The sensitivity analysis included the prediction of major osteoporotic fractures, single and multiple fractures, and the models were adjusted for the HR-pQCT measure and aBMD measured at 4 years instead of the baseline values. The receiver operating characteristic (ROC) curves were obtained from logistic regression models and areas under the ROC curves (AUCs) were compared using the nonparametric DeLong test.

Results

Comparison of men who were followed versus men who were lost to follow-up

Among the 825 patients recruited at baseline and aged ≥60, 734 (89%) had a HR-pQCT scan after 4 years and 91 (11%) did not. These 91 men were older and had more fractures (Table S1), and at baseline they had lower hip aBMD and poorer bone microarchitecture at both skeletal sites. All the differences became nonsignificant after adjustment for age.

Comparison of men who had incident fractures after 4 years versus men who did not

The median time to the first fracture was 51.6 months (IQR: 36.8; 85.4). Men who had fractures had lower aBMD at distal radius and hip and poorer bone microarchitecture at both skeletal sites (Table 1). Most of the differences were significant after adjustment for age. Men who had fractures had more rapid decrease in aBMD at the hip. At the distal radius, they had faster decreases in Tt.BMD, Ct.BMD, Ct.Th^d, Ct.Ar, Tb.BMD, inn.Tb.BMD, and Tb.Th^d. Most of the differences were significant after adjustment for age. The rates in change in the distal tibia HR-pQCT measures did not differ between men who did or did not have incident fractures.

Association between the rate of decrease in aBMD and fracture risk

Low baseline aBMD and more rapid decline at the femoral neck were both associated with higher fracture risk in multivariable models (HR = 1.71 per SD, 95% CI: 1.30–2.24 and HR = 1.58 per SD, 95% CI: 1.22–2.03, respectively, $p < .001$). Data were similar for total hip aBMD. At both the ROIs of the radius, baseline aBMD predicted fracture (e.g., ultradistal ROI: HR = 1.58 per SD, 95% CI: 1.25–2.00, $p < .001$), whereas the rate of bone loss did not.

Association between rate of distal radius bone microarchitecture decline and fracture risk

At the distal radius, a faster decrease in Tt.BMD was associated with a higher fracture risk (Table 2). The link was significant after adjustment for age, weight, prior fractures and falls, and baseline Tt.BMD. Further adjustment for the baseline value and the rate of change of ultradistal radius aBMD did not change the association. A faster decrease in Ct.BMD, Ct.Ar, and Ct.Th^d and a rapid increase in Tb.Ar were associated with a higher fracture risk after adjustment for the confounders, including the baseline HR-pQCT measures. The HRs were significant after further adjustment for ultradistal radius aBMD (baseline, rate of change). A faster decrease in Tb.Th^d, but not other trabecular measures, was associated with a higher fracture risk after adjustment for other variables, including ultradistal radius aBMD. A faster decline in Tb.BMD was associated with a higher fracture risk after adjustment for age, weight, prior falls and fractures, and the initial Tb.BMD value. However, the link became nonsignificant after further adjustment for the baseline value and the rate of change of ultradistal radius aBMD. The slopes of other HR-pQCT measures at the distal radius were not associated with fracture risk. The ultradistal radius aBMD (but not its loss) was significant regardless of the HR-pQCT measure (e.g., with Ct.BMD: HR = 1.41 per SD, 95% CI: 1.10–1.81, $p < .01$).

Table 1. Comparison of Values of aBMD and HR-oQCT Indices According to Fracture Occurring After 4 Years

	No fracture after 4 years ($n = 613$)	Fracture after 4 years ($n = 109$)	p Nonadjusted	p Adjusted for age
Age (years)	71.4 ± 7.0	72.8 ± 7.4	.06	
Weight (kg)	78.5 ± 11.4	78.2 ± 10.8	.82	
BMI (kg/m^2)	27.7 ± 3.6	27.5 ± 3.4	.77	
Fractures prior to baseline	114 (18%)	24 (22%)	.35	
Fractures over first 4 years	12 (11%)	41 (7%)	.10	
Falls prior to baseline	133 (20%)	14 (26%)	.28	.62
Areal bone mineral density (g/cm^2)				
Femoral neck	0.790 ± 0.128	0.740 ± 0.110	<.001	<.001
Total hip	0.965 ± 0.141	0.914 ± 0.125	<.001	<.005
Middistal radius	0.643 ± 0.076	0.615 ± 0.081	<.001	<.005
Ultradistal radius	0.464 ± 0.075	0.431 ± 0.071	<.001	<.001
Distal radius microarchitecture				
Tt.vBMD (mg/cm^3)	296.9 ± 65.2	272.4 ± 58.8	<.001	<.005
Ct.BMD (mg/cm^3)	803.6 ± 69.5	781.3 ± 75.7	<.001	<.05
Ct.Th (μm)	715.6 ± 225.2	636.8 ± 217.9	<.001	<.005
Ct.Ar (mm^2)	61.2 ± 17.7	54.9 ± 17.7	<.001	<.005
Tb.Ar (mm^2)	316.1 ± 66.3	329.6 ± 58.9	<.05	.10
Tb.BMD (mg/cm^3)	175.0 ± 40.2	162.7 ± 37.5	<.001	<.01
inn.Tb.BMD (mg/cm^3)	136.2 ± 42.1	125.1 ± 38.6	<.01	<.05
s.e.Tb.BMD (mg/cm^3)	231.4 ± 39.7	217.4 ± 38.3	<.001	<.005
Tb.N (1/mm)	1.87 ± 0.27	1.79 ± 0.28	<.005	<.01
Tb.Th (μm)	77.5 ± 12.2	75.3 ± 11.4	.07	.18
Tb.Sp (μm × 10^3)	468.5 ± 92.6	498.2 ± 109.3	<.005	<.01
Tb.1/N.SD (μm × 10^3)	207.3 ± 72.3	228.3 ± 117.6	<.01	<.05
Failure load (N)	2912 ± 640	2684 ± 689	<.005	<.01
Reaction force (N)	5615 ± 1291	5165 ± 1393	<.005	<.01
Distal tibia microarchitecture				
Tt.BMD (mg/cm^3)	291.4 ± 59.1	271.2 ± 48.5	<.001	<.005
Ct.BMD (mg/cm^3)	831.3 ± 64.4	814.7 ± 58.3	<.01	<.05
Ct.Th (μm)	1.19 ± 0.31	1.09 ± 0.27	<.001	<.005
Ct.Ar (mm^2)	135.7 ± 31.0	125.9 ± 29.4	<.001	<.005
Tb.Ar (mm^2)	697.0 ± 135.6	712.2 ± 118.7	.27	
Tb.BMD (mg/cm^3)	174.2 ± 38.4	164.2 ± 36.7	<.01	<.05
inn.Tb.BMD (mg/cm^3)	128.6 ± 40.8	116.8 ± 38.9	<.005	<.05
s.e.Tb.BMD (mg/cm^3)	241.4 ± 37.6	234.1 ± 36.1	.06	
Tb.N (1/mm)	1.74 ± 0.30	1.66 ± 0.30	<.01	<.05
Tb.Th (μm)	83.6 ± 13.5	82.5 ± 12.1	.42	
Tb.Sp (μm × 10^3)	509.5 ± 114.1	543.4 ± 146.4	<.01	<.05
Tb.1/N.SD (μm × 10^3)	245.9 ± 89.9	277.4 ± 188.1	<.01	<.01
Failure load (N)	7430 ± 1244	7004 ± 1278	<.005	<.01
Reaction force (N)	14764 ± 2624	13895 ± 2694	<.005	<.05
Difference in areal bone mineral density (mg/cm^2) between value at 4 years and value at baseline				
Femoral neck	−11.46 ± 30.93	−21.02 ± 33.25	<.005	<.05
Total hip	−2.26 ± 32.00	−10.90 ± 32.01	<.05	<.05
Middistal radius	−11.70 ± 19.54	−11.70 ± 19.06	.98	
Ultradistal radius	−6.16 ± 18.10	−5.76 ± 19.03	.84	
Difference in HR-pQCT indices at distal radius between value at 4 years and value at baseline				
Tt.BMD (mg/cm^3)	−5.79 ± 10.98	−9.45 ± 17.57	<.01	<.05
Ct.BMD (mg/cm^3)	−14.23 ± 22.17	−20.90 ± 24.10	<.005	<.05
Ct.Th (μm)	−36.25 ± 56.11	−48.37 ± 55.33	<.05	<.05
Ct.Ar (mg/cm^3)	−3.00 ± 4.35	−4.20 ± 5.47	<.05	<.05
Tb.Ar (mm^2)	2.13 ± 3.55	2.89 ± 4.04	.06	.10
Tb.BMD (mg/cm^3)	−0.10 ± 5.05	−1.47 ± 9.46	<.05	.06
inn.Tb.BMD (mg/cm^3)	−0.04 ± 5.05	−1.28 ± 8.72	<.05	.08
s.e.Tb.BMD (mg HA/cm^3)	−0.19 ± 6.34	−1.72 ± 11.30	.06	.09
Tb.N (1/mm × 10^3)	24.9 ± 141.3	41.2 ± 126.3	.28	
Tb.Th (μm)	−1.06 ± 5.69	−2.42 ± 5.72	<.05	<.05
Tb.Sp (μm)	−5.70 ± 36.48	−9.31 ± 36.62	.36	

(Continues)

Table 1. Continued

	No fracture after 4 years ($n = 613$)	Fracture after 4 years ($n = 109$)	p Nonadjusted	p Adjusted for age
Tb.1/N.SD (μm × 10^3)	−0.28 ± 23.79	3.79 ± 37.73	.15	
Failure load (N)	−92 ± 199	−110 ± 217	.45	
Reaction force (N)	−188 ± 422	−235 ± 451	.34	
Difference in HR-pQCT indices at distal tibia between 4 years and baseline				
Tt.BMD (mg/cm^3)	−3.49 ± 9.66	−4.73 ± 8.21	.21	
Ct.BMD (mg/cm^3)	−11.18 ± 19.35	−13.72 ± 17.32	.21	
Ct.Th (μm)	−35.86 ± 81.23	−48.79 ± 73.57	.12	
Ct.Ar (mm^2)	−3.88 ± 8.58	−5.27 ± 8.45	.11	
Tb.Ar (mm^2)	2.25 ± 6.88	3.51 ± 7.32	.08	.27
Tb.BMD (mg/cm^3)	0.25 ± 3.47	−0.02 ± 3.50	.88	
inn.Tb.BMD (mg/cm^3)	−0.87 ± 3.73	−1.41 ± 4.08	.19	
s.e.Tb.BMD (mg/cm^3)	1.90 ± 4.20	2.01 ± 3.94	.82	
Tb.N (1/mm × 10^3)	42.5 ± 151.7	34.1 ± 143.7	.61	
Tb.Th (μm)	−1.63 ± 6.88	−1.34 ± 6.55	.70	
Tb.Sp (μm)	−10.49 ± 43.62	−9.73 ± 44.79	.77	
Tb.1/N.SD (μm × 10^3)	−2.94 ± 25.31	1.26 ± 27.70	.10	
Failure load (N)	−181 ± 316	−216 ± 261	.29	
Reaction force (N)	−402 ± 726	−453 ± 589	.50	

Note: The results are presented as mean ± SD.

Abbreviations: Tt.BMD, total volumetric bone mineral density (BMD); Ct.BMD, cortical volumetric BMD; Ct.Ar, cortical area; Ct.Th[d], cortical thickness; Tb.Ar, trabecular area; Tb.BMD, trabecular volumetric BMD; s.e.Tb.BMD, subendocortical (outer) Tb.BMD; inn.Tb.BMD, inner (central) Tb.BMD; Tb.N, trabecular number; Tb.Th[d], trabecular thickness; Tb.Sp[d], trabecular separation; Tb.1/N.SD, heterogeneity of trabecular separation.

Table 2. Association of Bone Microarchitecture Deterioration at Distal Radius with Risk of Fracture

	Incident fracture after 4 years				
Difference in HR-pQCT measure between 4 years and baseline Distal radius (per SD decrease)	Not adjusted	Adjusted for age, weight, prevalent fractures, and prior falls	Additionally adjusted for value of HR-pQCT measure at baseline	Additionally adjusted for aBMD (baseline + change over first 4 years) Ultradistal radius	Additionally adjusted for aBMD (baseline + change over first 4 years) Distal radius
Tt.BMD	1.41 (1.19–1.66)***	1.34 (1.14–1.58)***	1.41 (1.19–1.68)***	1.48 (1.16–1.89)**	1.53 (1.20–1.95)***
Ct.BMD	1.47 (1.22–1.77)***	1.37 (1.14–1.65)***	1.36 (1.12–1.64)**	1.35 (1.09–1.67)**	1.38 (1.11–1.72)**
Ct.Ar	1.39 (1.15–1.67)***	1.32 (1.09–1.59)**	1.36 (1.12–1.65)**	1.37 (1.09–1.73)**	1.42 (1.12–1.79)**
Ct.Th[d]	1.41 (1.16–1.73)***	1.35 (1.11–1.65)**	1.42 (1.15–1.74)**	1.43 (1.11–1.84)**	1.48 (1.15–1.90)**
Tb.Ar[a]	1.34 (1.11–1.62)**	1.31 (1.09–1.58)**	1.33 (1.00–1.61)**	1.37 (1.09–1.72)**	1.36 (1.09–1.70)**
Tb.BMD	1.31 (1.12–1.54)***	1.23 (1.05–1.43)**	1.24 (1.05–1.46)*	1.22 (0.95–1.57)	1.23 (0.96–1.57)
s.e.Tb.BMD	1.29 (1.07–1.54)**	1.19 (1.01–1.42)*	1.22 (1.02–1.46)*	1.15 (0.91–1.46)	1.15 (0.91–1.45)
inn.Tb.BMD	1.32 (1.11–1.57)**	1.25 (1.06–1.46)**	1.24 (1.04–1.47)*	1.22 (0.95–1.58)	1.24 (0.96–1.59)
Tb.N	0.91 (0.75–1.11)	0.86 (0.71–1.05)	0.93 (0.75–1.14)	0.88 (0.69–1.09)	0.89 (0.71–1.11)
Tb.Th[d]	1.26 (1.03–1.54)*	1.32 (1.08–1.61)**	1.45 (1.16–1.81)**	1.26 (1.01–1.59)*	1.34 (1.07–1.68)*
Tb.Sp[d][a]	1.09 (0.89–1.33)	1.12 (0.92–1.36)	1.04 (0.86–1.26)	1.08 (0.87–1.33)	1.06 (0.86–1.32)
Tb.1/N.SD[a]	1.15 (0.99–1.34)	1.11 (0.94–1.30)	1.11 (0.96–1.28)	1.11 (0.94–1.29)	1.12 (0.95–1.31)
Failure load	1.17 (0.94–1.45)	1.17 (0.94–1.46)	1.16 (0.93–1.44)	1.03 (0.80–1.32)	1.16 (0.92–1.46)
Reaction force	1.18 (0.95–1.47)	1.18 (0.95–1.48)	1.18 (0.96–1.47)	1.05 (0.82–1.34)	1.19 (0.94–1.49)

Note: The results are presented as HR (95% confidence interval).

Abbreviations: Tt.BMD, total volumetric bone mineral density (vBMD); Ct.BMD, cortical vBMD; Ct.Ar, cortical area; Ct.Th[d], cortical thickness; Tb.Ar, trabecular area; Tb.BMD, trabecular vBMD; s.e.Tb.BMD, subendocortical (outer) Tb.BMD; inn.Tb.BMD, inner (central) Tb.BMD; Tb.N, trabecular number; Tb.Th[d], trabecular thickness; Tb.Sp[d], trabecular separation; Tb.1/N.SD, heterogeneity of trabecular separation.

[a]per SD increase.

*$p < .05$.

**$p < .01$.

***$p < .001$.

Results were similar after adjustment for distal radius aBMD (baseline, change). Faster decreases in Tt.BMD (HR = 1.53 per SD, 95% CI: 1.20–1.95, $p < .001$) and Ct.Th[d] were both associated with a higher risk of fracture. The baseline distal radius aBMD was significant in only a few models (e.g., with Tb.Ar: HR = 1.32 per SD increase, 95% CI: 1.11–1.57, $p < .005$).

Association between rate of distal tibia bone microarchitecture decline and fracture risk

At the distal tibia, faster decreases in Tt.BMD, Ct.BMD, Ct.Ar, Ct.Th^{d}, and the failure load, as well as a more rapid increase in Tb.Ar, were associated with a higher fracture risk (Table 3). However, all the associations became nonsignificant after adjustment for confounders. Femoral neck aBMD and bone loss were significant in the final models with each HR-pQCT measure (e.g., with Ct.Th^{d}: HR = 1.47 per SD, 95% CI: 1.10–1.96, $p < .01$ and HR = 1.51 per SD, 95% CI: 1.15–1.99, $p < 0.005$, respectively). Similarly, total hip aBMD and bone loss remained significant in the final models with most of the HR-pQCT measures.

Single versus multiple fractures

Ninety-five men had one incident fracture, whereas 14 men sustained at least two fractures. In the fully adjusted models, a rapid decrease in the distal radius Tt.BMD, Ct.BMD, Ct.Th^{d}, and Ct.Ar and accelerated Tb.Ar expansion were each associated with a higher risk of one fracture (e.g., Tt.BMD: HR = 1.36 per SD, 95% CI: 1.06–1.75, $p < .05$), whereas the decrease in ultradistal aBMD was not (Fig. 1). By contrast, both the changes in the aforementioned HR-pQCT measures and the decrease in the ultradistal aBMD were associated with a higher risk of multiple fractures, e.g., aBMD (HR = 2.47 per SD, 95% CI: 1.30–4.70, $p < .01$) and Tb.Ar (HR = 2.71 per SD, 95% CI: 1.31–5.61, $p < .01$). Other HR-pQCT measures were not associated with the risk of one or multiple fractures. The results were similar after adjustment for distal radius aBMD. Distal tibia HR-pQCT measures were not associated with a risk of single or multiple fractures.

Major osteoporotic fractures

Forty-eight men sustained incident major osteoporotic fractures (MOFs). At the distal radius, a rapid decrease in Tt.BMD, Ct.BMD, Ct.Ar, Ct.Th^{d}, and inn.Tb.BMD and a rapid increase in Tb.Ar and Tb.1/N.SD were associated with a higher risk of MOF (Fig. 2). Other indices did not predict the MOFs. The results were similar after adjustment for distal radius aBMD. Distal tibia HR-pQCT measures were not associated with a risk of MOF.

All fractures

The patterns were similar to the analysis focused on fragility fractures, but the HR values were lower for the radius HR-pQCT measures and nonsignificant for the distal tibia. For instance, in the fully adjusted model including distal radius aBMD, a lower distal radius Tt.BMD was associated with a higher risk for all fractures (HR = 1.48 per SD, 95% CI: 1.15–1.89, $p < .005$).

Analyses adjusted for follow-up values of aBMD and HR-pQCT indices

The models were adjusted for the ultradistal radius aBMD and the distal radius HR-pQCT measures taken after 4 years instead of at baseline. Changes in Tt.BMD, cortical measures, and Tb.Ar were significantly associated with a higher fracture risk (e.g., Tt.BMD: HR = 1.37 per SD, 95% CI: 1.11–1.69, $p < .005$; Ct.Th: HR = 1.32 per SD, 95% CI: 1.07–1.64, $p < .01$; Tb.Ar: HR = 1.35 per SD, 95% CI: 1.08–1.70, $p < .01$). In similar models, changes in Tt.BMD, cortical measures, and Tb.Ar were significantly associated with a higher risk of MOF (e.g., Tt.BMD: HR = 1.61 per SD,

Table 3. Association of Bone Microarchitecture Deterioration at Distal Tibia with Risk of Fracture

	Incident fracture after 4 years				
Difference in HR-pQCT measure between 4 years and baseline Distal tibia (per SD decrease)	Not adjusted	Adjusted for age, weight, prevalent fractures, and prior falls	Additionally adjusted for value of HR-pQCT measure at baseline	Additionally adjusted for aBMD (baseline + change over first 4 years) Femoral neck	Additionally adjusted for aBMD (baseline + change over first 4 years) Hip
Tt.BMD	1.29 (1.06–1.57)*	1.16 (0.95–1.40)	1.16 (0.96–1.41)	1.07 (0.87–1.33)	1.08 (0.87–1.34)
Ct.BMD	1.35 (1.14–1.61)***	1.19 (0.98–1.44)	1.18 (0.97–1.43)	1.08 (0.87–1.34)	1.07 (0.85–1.34)
Ct.Ar	1.33 (1.11–1.59)**	1.17 (0.97–1.42)	1.18 (0.98–1.42)	1.09 (0.89–1.32)	1.08 (0.88–1.32)
Ct.Th^{d}	1.35 (1.14–1.61)***	1.19 (0.99–1.44)	1.19 (0.99–1.44)	1.09 (0.88–1.35)	1.07 (0.86–1.34)
Tb.Ar[a]	1.19 (1.03–1.38)*	1.13 (0.95–1.33)	1.14 (0.96–1.36)	1.06 (0.86–1.30)	1.05 (0.85–1.29)
Tb.BMD	1.01 (0.86–1.19)	1.02 (0.87–1.20)	1.04 (0.87–1.25)	1.01 (0.82–1.25)	1.00 (0.81–1.24)
s.e.Tb.BMD	1.08 (0.84–1.40)	1.03 (0.83–1.28)	1.02 (0.81–1.28)	1.05 (0.82–1.33)	1.05 (0.83–1.33)
inn.Tb.BMD	1.04 (0.91–0.19)	1.05 (0.91–1.20)	1.07 (0.91–1.25)	1.04 (0.86–1.25)	1.03 (0.85–1.24)
Tb.N	0.95 (0.78–1.16)	0.97 (0.79–1.19)	0.93 (0.75–1.16)	0.98 (0.79–1.22)	0.98 (0.79–1.21)
Tb.Th^{d}	0.96 (0.78–1.18)	0.99 (0.81–1.21)	1.01 (0.82–1.24)	1.01 (0.83–1.25)	0.99 (0.81–1.23)
Tb.Sp^{da}	1.02 (0.83–1.26)	1.02 (0.82–1.27)	1.03 (0.85–1.25)	1.00 (0.83–1.22)	1.01 (0.83–1.22)
Tb.1/N.SD[a]	1.18 (0.99–1.40)	1.17 (0.96–1.42)	1.10 (0.92–1.33)	1.04 (0.87–1.24)	1.06 (0.89–1.26)
Failure load	1.23 (1.00–1.51)*	1.19 (0.98–1.42)	1.12 (0.92–1.37)	1.02 (0.83–1.27)	1.02 (0.82–1.26)
Reaction force	1.19 (0.97–1.46)	1.16 (0.95–1.42)	1.11 (0.91–1.36)	1.02 (0.83–1.25)	1.02 (0.83–1.25)

Note: The results are presented as HR (95% confidence interval).

Abbreviations: Tt.BMD, total volumetric bone mineral density (vBMD); Ct.BMD, cortical vBMD; Ct.Ar, cortical area; Ct.Th^{d}, cortical thickness; Tb.Ar, trabecular area; Tb.BMD, trabecular vBMD; s.e.Tb.BMD, subendocortical (outer) Tb.BMD; inn.Tb.BMD, inner (central) Tb.BMD; Tb.N, trabecular number; Tb.Th^{d}, trabecular thickness; Tb.Sp^{d}, trabecular separation; Tb.1/N.SD, heterogeneity of trabecular separation.

[a]per SD increase.

*$p < .05$.

*$p < .01$.

***$p < .001$.

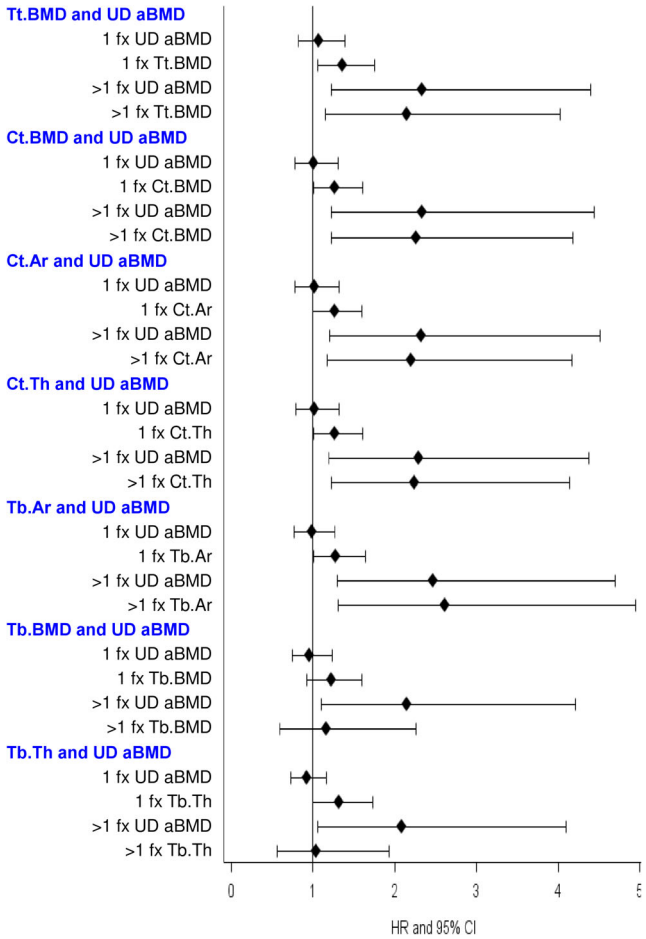

Fig. 1. Associations of rates of change in ultradistal radius aBMD (UD aBMD) measured by DXA and in selected HR-pQCT measures at distal radius with risk of one fracture (1 fx) and with risk of multiple fractures (>1 fx) in older men. The figure presents the HR values per one standard deviation change (increase in Tb.Ar or decrease for other variables) and 95% CI for HR-pQCT measures. The figure presents only HR for the rates of change in aBMD and in the bone microarchitecture measures. HR values for the baseline values of aBMD or the HR-pQCT measures are not presented. Tt.BMD, total volumetric bone mineral density; Ct.BMD, cortical BMD; Ct.Ar, cortical area; Ct.Th, cortical thickness; Tb.Ar, trabecular area; Tb.BMD, trabecular BMD; Tb.Th, trabecular thickness.

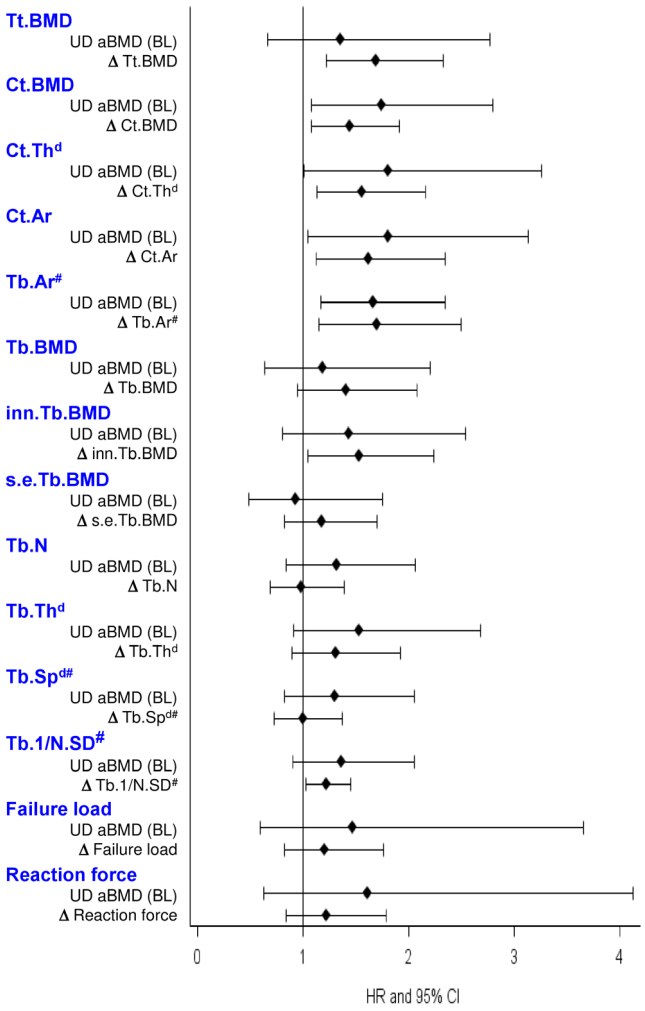

Fig. 2. Associations of ultradistal radius aBMD at baseline (UD aBMD BL) and of rates of change (described using Greek letter delta, Δ) in HR-pQCT measures at distal radius with risk of major osteoporotic fracture in older men. The figure presents only the HR per one standard deviation (SD) decrease in baseline ultradistal radius aBMD and per one SD rate of change of the HR-pQCT measures (increase in Tb.Ar, Tb.Sp, Tb.1/N.SD or decrease for other variables) as well as corresponding 95% CI. HR values for rate of change in ultradistal radius aBMD and baseline values of HR-pQCT measures are not presented. Tt.BMD, total volumetric bone mineral density; Ct.BMD, cortical BMD; Ct.Th^{d}, cortical thickness; Ct.Ar, cortical area; Tb.Ar, trabecular area; Tb.BMD, trabecular BMD; inn.Tb.BMD, inner (central) Tb.BMD; s.e.Tb.BMD, subendocortical (outer) Tb.BMD; Tb.N, trabecular number; Tb.Th^{d}, trabecular thickness; Tb.Sp^{d}, trabecular separation; Tb.1/N.SD, heterogeneity of trabecular separation. #For these variables, HR is calculated per SD increase.

95% CI: 1.20–2.17, $p < .005$; Ct.Ar: HR = 1.63 per SD, 95% CI: 1.17–2.29, $p < .005$; Tb.Ar: HR = 1.64 per SD, 95% CI: 1.17–2.32, $p < .005$).

Exclusion of men who had an incident fracture during first 4 years

Because a fracture may trigger bone loss, we excluded 53 men who had had a fracture during the first 4 years. In the remaining 679 men, 97 had incident fractures after the 4-year follow-up. The results were similar to those in the entire cohort. Rapid changes in distal radius Tt.BMD, Ct.BMD, Ct.Ar, Ct.Th^{d}, and Tb.Ar and a low baseline ultradistal radius aBMD were associated with a high fracture risk, e.g., a decrease in Ct.Th^{d} (HR = 1.37 per SD, 95% CI: 1.04–1.80, $p < .05$ and baseline aBMD: HR = 1.64 per SD, 95% CI: 1.13–2.39; $p < .01$). The results were similar after adjustment for distal radius aBMD.

ROC analyses and comparison of AUC for fragility fractures

The reference model included age, weight, prior falls and fractures, baseline and slope of aBMD (ultradistal radius for the radius, femoral neck for the tibia), and HR-pQCT measure at baseline. Further addition of the slope of the HR-pQCT measure did

not increase the AUC significantly. The largest increase was found for the distal radius Ct.Th^d and Tb.Ar (from 0.66 to 0.69), which was not significant ($p = .50$). The findings were similar for the radius after adjustment for distal radius aBMD and for the tibia after adjustment for total hip aBMD.

Discussion

In older men followed prospectively for 12 years, faster bone loss at the distal radius (Tt.BMD, cortical bone, Tb.Th^d) over 4 years was associated with a higher fracture risk. This association was significant after adjustment for confounders including baseline values of aBMD, the HR-pQCT measure, and the DXA-measured bone loss. However, assessment of the decline in bone microarchitecture did not improve the fracture prediction in this cohort.

In the models without HR-pQCT measures, baseline aBMD and bone loss at the hip predicted fractures. By contrast, in the models that included distal radius aBMD, only baseline aBMD, but not bone loss, was associated with the fracture risk. Previously, both initial aBMD and bone loss at the hip were associated with the fracture risk in most,[9,11-14,17,22-24] but not all,[16,19] studies. Data on the link between bone loss at the distal radius and the fracture risk are discordant. This may be due to poor statistical power. In our study, the average percentage bone loss was similar at the forearm and the hip, and rates of bone loss at the radius were similar in both groups. However, distal radius ROIs are small and may be sensitive to positioning error, so bone loss at the radius may be difficult to assess in short-term follow-ups. The link between the rate of bone loss and fracture risk has been detected in long-term follow-ups,[10,25] but not always in short-term follow-ups,[20,21] similar to our study.

The rates of change of some HR-pQCT measures of distal radius predicted fractures, whereas those at the distal tibia did not. In our previous analysis, baseline values of the distal tibia HR-pQCT measures did not predict incident fracture either.[5] In the models that included aBMD and a HR-pQCT measure, only bone loss at the hip, not that of the ultradistal/distal radius, was predictive of fractures. Thus, it is plausible that only the strongest predictors may remain significant in multivariable models.

In most HR-pQCT studies to date, both cortical and trabecular indices predicted fractures.[8] Biomechanical studies also show that the trabecular bone structure deterioration confers higher bone fragility.[35] By contrast, in our study, mainly the changes in the cortical indices predicted fracture. Prospective estimation of trabecular bone decline by HR-pQCT may not be accurate because of the cortical bone trabecularization and resolution limitations of the first-generation HR-pQCT. The change in the distal radius Tb.Th^d was associated with fracture. Because it is a derived measure and not directly measured (in first-generation HR-pQCT), the data should be interpreted cautiously. The lack of a link between the μFE measures and fracture risk is counterintuitive, given findings showing that μFE-derived measures are a good predictor of fracture risk.[7] Our algorithms assess the resistance to compression. However, the resistance to other deformations (bending, torsion) may be more important. They reflect overall bone strength and do not account for bone morphology or composition.[36]

Low aBMD and poor bone microarchitecture are associated with higher fracture risk.[5-9] The repeated measures allow for the assessment of bone loss on bone fragility. A faster bone decline results in poor bone status, e.g., faster prior bone loss was associated with poorer bone microarchitecture at the distal radius and distal tibia after adjustment for the confounders, including final femoral neck aBMD.[26] Greater bone loss also results in subsequent lower aBMD associated with a higher fracture risk. The link between bone loss and fracture risk was stronger in men with a higher initial aBMD than in men with a lower aBMD.[22] Men with rapid bone loss may have entered the zone of low aBMD and high fracture risk, whereas men with stable aBMD remained in the zone of low fracture risk. Similarly, women who transitioned to lower aBMD category (e.g., osteopenia to osteoporosis) had higher fracture risk than those who remained in the same group regardless of the initial category.[37]

Rapid bone loss results in a lower aBMD; however, it may also be a risk factor per se. In our cohort, faster bone decline at the distal radius was associated with a higher risk of fracture after adjustment for the final values of aBMD and of the HR-pQCT measures, but the point estimates were lower than in the models adjusted for the initial values. Lower HR values and the loss of statistical significance after adjustment for the final values in prior studies[9,21] suggest that rapid bone loss increases the fracture risk because of the poorer bone status at the end of the initial follow-up. However, rapid bone loss also predicted hip fracture after adjustment for the final aBMD.[9] Thus, rapid bone loss may result in a bone nonadapted to the subject's body habitus, physical activity, or mechanical strains. Cortical bone loss may also be correlated with parallel bone decline, which is not detected by HR-pQCT but increases bone fragility, e.g., trabecular structural decline or the deterioration of the bone matrix or mineral lattice.[36]

The improvement in fracture prediction by repeated DXA measures is not certain. The precision of DXA or HR-pQCT versus individual changes is poor. Bone status should be assessed over an extended follow-up (which delays treatment) or at sites with low variability. In women, bone loss at the lumbar spine (with signal-to-noise ratio [SNR]: 2.5) predicted fractures, whereas that at the femoral neck (SNR: 1.5) did not.[18] It is not clear whether an assessment of the change in bone status would provide additional information on the fracture risk. The inclusion of bone loss (aBMD) in the model did not improve fracture prediction.[12-14,17,22] This pattern was found in both sexes regardless of the site of DXA measurement and regardless of the type of fracture. We show that the repeated HR-pQCT measures do not improve fracture prediction in men. Thus, it does not seem useful to incorporate repeated measurements of aBMD or of standard measures from first-generation HR-pQCT into the screening strategy to assess fracture risk in older men. However, recent data show that the link between bone characteristics and fracture risk varies according to the bone phenotype.[38] Whether the utility of the repeated measures varies according the phenotype needs further investigation.

A strength of the study includes that bone microarchitecture was assessed at the non-weight-bearing radius and the weight-bearing tibia using a reference device (in 2006). The incident fractures were confirmed by DXA spine scans or by a medical professional, and trauma level of the fractures was assessed.

We recognize the study's limitations. The cohort of this single-center study was of modest size and consisted primarily of Caucasian men. Older volunteers for epidemiologic studies are typically healthier than their peers. Men who did not return after 4 years were older and had more fractures at baseline. Thus, bone decline and the number of incident fractures may have been underestimated. The number of incident fractures was

not sufficient to analyze vertebral or hip fractures separately. The results cannot be extrapolated to women, young men, or other ethnic groups. In terms of imaging, partial volume effects may bias bone microarchitecture evaluation. Trabecularization of cortical bone results in the overestimation of cortical bone loss while underestimating trabecular bone loss. Tb.Th^{d}, Tb.1/N.SD, and Ct.Th^{d} are derived, not measured. For some HR-pQCT measures (e.g., Tb.N, Tb.Th^{d}, Tb.1/N.SD), LSC and SNR are relatively large compared the observed changes. These two factors likely contributed to the lack of association between the changes in trabecular measures and the risk of fracture. HR-pQCT does not assess the intrinsic bone decline (microdamage, post-translational modifications of bone proteins, mineral imperfections). Self-reported prior fractures and falls were not checked.

In summary, in older men followed prospectively, a faster decline in cortical bone at the distal radius was associated with a higher fracture risk after adjustment for relevant confounders. This link was stronger for MOFs and multiple fractures. Of note, faster cortical bone loss was related to increased fracture risk after adjustment for the baseline value and after adjustment for the follow-up value. This suggests that rapid cortical bone loss (e.g., distal radius Ct.Th^{d}) is associated with high bone fragility regardless of the value of the HR-pQCT measure at a single time point. However, repeated HR-pQCT measures did not improve fracture prediction. Thus, utility of repeated measures of aBMD or HR-pQCT for the screening strategy (e.g., the XtremeCT II device) in older men needs further study.

Funding Information

This study was supported by grants from Roche pharmaceutical company, Basel, Switzerland, Agence Nationale de la Recherche (ANR-07-PHYSIO-023, ANR-10-BLAN-1137), Abondement ANVAR (E1482.042), and Hospices Civils de Lyon (50564). The supporting sponsors played no role in the study design or the collection, analysis, or interpretation of data.

Conflict of Interest Statement

All the authors declare that they have no conflict of interest concerning this manuscript.

Author Contributions

Elina Gunsing: Formal analysis; data curation; writing – original draft. **Philippe P. Wagner:** Formal analysis; data curation. **Danielle E. Whittier:** Data curation; software; methodology; formal analysis. **Steven K. Boyd:** Methodology; supervision; writing – review and editing; conceptualization. **Roland Chapurlat:** Conceptualization; funding acquisition; writing – review and editing; validation. **Pawel Szulc:** Conceptualization; investigation; funding acquisition; writing – review and editing; validation; project administration; supervision.

Data Availability Statement

Research data are not shared.

References

1. Rachner TD, Khosla S, Hofbauer LC. Osteoporosis: now and the future. Lancet. 2011;377:1276–1287. https://doi.org/10.1016/S0140-6736(10)62349-5
2. Szulc P, Munoz F, Duboeuf F, Marchand F, Delmas PD. Bone mineral density predicts osteoporotic fractures in elderly men: the MINOS study. Osteoporos Int. 2005;16:1184–1192. https://doi.org/10.1007/s00198-005-1970-9.
3. Cummings SR, Cawthon PM, Ensrud KE, Cauley JA, Fink HA, Orwoll ES. BMD and risk of hip and nonvertebral fractures in older men: a prospective study and comparison with older women. J Bone Miner Res. 2006;21:1550–1556. https://doi.org/10.1359/jbmr.060708.
4. Bouxsein ML. Technology insight: noninvasive assessment of bone strength in osteoporosis. Nat Clin Pract Rheumatol. 2008;4:310–318. https://doi.org/10.1038/ncprheum0798.
5. Szulc P, Boutroy S, Chapurlat R. Prediction of fractures in men using bone microarchitectural parameters assessed by high-resolution peripheral quantitative computed tomography - the prospective STRAMBO study. J Bone Miner Res. 2018;33:1470–1479. https://doi.org/10.1002/jbmr.3451
6. Langsetmo L, Peters KW, Burghardt AJ, et al. Volumetric bone mineral density and failure load of distal limbs predict incident clinical fracture independent of FRAX and clinical risk factors among older men. J Bone Miner Res. 2018;33:1302–1311. https://doi.org/10.1002/jbmr.3433
7. Samelson EJ, Broe KE, Xu H, et al. Cortical and trabecular bone microarchitecture as an independent predictor of incident fracture risk in older women and men in the Bone Microarchitecture International Consortium (BoMIC): a prospective study. Lancet Diabetes Endocrinol. 2019;7:34–43. https://doi.org/10.1016/S2213-8587(18)30308-5.
8. Mikolajewicz N, Bishop N, Burghardt AJ, et al. HR-pQCT measures of bone microarchitecture predict fracture: systematic review and meta-analysis. J Bone Miner Res. 2020;35:446–459. https://doi.org/10.1002/jbmr.3901.
9. Cawthon PM, Ewing SK, MacKey DC, et al. Change in hip bone mineral density and risk of subsequent fractures in older men. J Bone Miner Res. 2012;27:2179–2188. https://doi.org/10.1002/jbmr.1671
10. Sornay-Rendu E, Munoz F, Duboeuf F, Delmas PD. Rate of forearm bone loss is associated with an increased risk of fracture independently of bone mass in postmenopausal women: the OFELY study. J Bone Miner Res. 2005;20:1929–1935. https://doi.org/10.1359/JBMR.050704.
11. Nguyen TV, Center JR, Eisman JA. Femoral neck bone loss predicts fracture risk independent of baseline BMD. J Bone Miner Res. 2005;20:1195–1201. https://doi.org/10.1359/jbmr.050215.
12. Berger C, Langsetmo L, Joseph L, et al. Association between change in BMD and fragility fracture in women and men. J Bone Miner Res. 2009;24:361–370. https://doi.org/10.1359/jbmr.081004.
13. Crandall CJ, Larson J, Wright NC, et al. Serial bone density measurement and incident fracture risk discrimination in postmenopausal women. JAMA Internal Med. 2020;180:1232–1240. https://doi.org/10.1001/jamainternmed.2020.2986.
14. Berry SD, Samelson EJ, Pencina MJ, et al. Repeat bone mineral density screening and prediction of hip and major osteoporotic fracture. JAMA. 2013;310:1256–1262. https://doi.org/10.1001/jama.2013.277817.
15. Leslie WD, Brennan-Olsen SL, Morin SN, Lix LM. Fracture prediction from repeat BMD measurements in clinical practice. Osteoporos Int. 2016;27:203–210. https://doi.org/10.1007/s00198-015-3259-y.
16. Leslie WD, Morin SN, Lix LM. Rate of bone density change does not enhance fracture prediction in routine clinical practice. J Clin Endocrinol Metab. 2012;97:1211–1218. https://doi.org/10.1210/jc.2011-2871.
17. Hillier TA, Stone KL, Bauer DC, et al. Evaluating the value of repeat bone mineral density measurement and prediction of fractures in older women: the study of osteoporotic fractures. Arch Intern Med. 2007;167:155–160. https://doi.org/10.1001/archinte.167.2.155.
18. Shieh A, Karlamangla AS, Huang MH, Han W, Greendale GA. Faster lumbar spine bone loss in midlife predicts subsequent fracture

independent of starting bone mineral density. J Clin Endocrinol Metab. 2021;106:e2491–e2501. https://doi.org/10.1210/clinem/dgab279.

19. Bruyere O, Varela AR, Adami S, et al. Loss of hip bone mineral density over time is associated with spine and hip fracture incidence in osteoporotic postmenopausal women. Eur J Epidemiol. 2009;24:707–712. https://doi.org/10.1007/s10654-009-9381-4.
20. Gnudi S, Malavolta N, Lisi L, Ripamonti C. Bone mineral density and bone loss measured at the radius to predict the risk of nonspinal osteoporotic fracture. J Bone Miner Res. 2001;16:1130–1135. https://doi.org/10.1359/jbmr.2001.16.6.1130.
21. Ahmed LA, Emaus N, Berntsen GK, et al. Bone loss and the risk of nonvertebral fractures in women and men: the Tromsø study. Osteoporos Int. 2010;21:1503–1511. https://doi.org/10.1007/s00198-009-1102-z.
22. Ensrud KE, Lui LY, Crandall CJ, et al. Repeat bone mineral density screening measurement and fracture prediction in older men: a prospective cohort study. J Clin Endocrinol Metab. 2022;107:e3877–e3886. https://doi.org/10.1210/clinem/dgac324.
23. Fujiwara S, Kasagi F, Masunari N, Naito K, Suzuki G, Fukunaga M. Fracture prediction from bone mineral density in Japanese men and women. J Bone Miner Res. 2003;18:1547–1553. https://doi.org/10.1359/jbmr.2003.18.8.1547.
24. Crandall CJ, Hovey KM, Andrews CA, et al. Bone mineral density as a predictor of subsequent wrist fractures: findings from the women's health initiative study. J Clin Endocrinol Metab. 2015;100:4315–4324. https://doi.org/10.1210/jc.2015-2568.
25. Riis BJ, Hansen MA, Jensen AM, Overgaard K, Christiansen C. Low bone mass and fast rate of bone loss at menopause: equal risk factors for future fracture: a 15-year follow-up study. Bone. 1996;19:9–12. https://doi.org/10.1016/8756-3282(96)00102-0.
26. Cauley JA, Burghardt AJ, Harrison SL, et al. Accelerated bone loss in older men: effects on bone microarchitecture and strength. J Bone Miner Res. 2018;33:1859–1869. https://doi.org/10.1002/jbmr.3468.
27. Szulc P, Boutroy S, Vilayphiou N, Chaitou A, Delmas PD, Chapurlat R. Cross-sectional analysis of the association between fragility fractures and bone microarchitecture in older men: the STRAMBO study. J Bone Miner Res. 2011;26:1358–1367. https://doi.org/10.1002/jbmr.319.
28. Whittier DE, Boyd SK, Burghardt AJ, et al. Guidelines for the assessment of bone density and microarchitecture in vivo using high-resolution peripheral quantitative computed tomography. Osteoporos Int. 2020;31:1607–1627. https://doi.org/10.1007/s00198-020-05438-5.
29. Chaitou A, Boutroy S, Vilayphiou N, et al. Association between bone turnover rate and bone microarchitecture in men: the STRAMBO study. J Bone Miner Res. 2010;25:2313–2323. https://doi.org/10.1002/jbmr.124.
30. Buie HR, Campbell GM, Klinck RJ, MacNeil JA, Boyd SK. Automatic segmentation of cortical and trabecular compartments based on a dual threshold technique for in vivo micro-CT bone analysis. Bone. 2007;41:505–515. https://doi.org/10.1016/j.bone.2007.07.007.
31. Pialat JB, Burghardt AJ, Sode M, Link TM, Majumdar S. Visual grading of motion induced image degradation in high resolution peripheral computed tomography: impact of image quality on measures of bone density and micro-architecture. Bone. 2012;50:111–118. https://doi.org/10.1016/j.bone.2011.10.003
32. MacNeil JA, Boyd SK. Bone strength at the distal radius can be estimated from high-resolution peripheral quantitative computed tomography and the finite element method. Bone. 2008;42:1203–1213. https://doi.org/10.1016/j.bone.2008.01.017
33. Pistoia W, Van Rietbergen B, Lochmüller EM, Lill CA, Eckstein F, Rüegsegger P. Image-based micro-finite-element modeling for improved distal radius strength diagnosis: moving from "bench" to "bedside". J Clin Densitom. 2004;7:153–160. https://doi.org/10.1385/jcd:7:2:153
34. Szulc P, Munoz F, Marchand F, Delmas PD. Semiquantitative evaluation of prevalent vertebral deformities in men and their relationship with osteoporosis: the MINOS study. Osteoporos Int. 2001;12:302–310. https://doi.org/10.1007/s001980170120
35. Pialat JB, Vilayphiou N, Boutroy S, et al. Local topological analysis at the distal radius by HR-pQCT: application to in vivo bone microarchitecture and fracture assessment in the OFELY study. Bone. 2012;51:362–368. https://doi.org/10.1016/j.bone.2012.06.008.
36. Bolger MW, Romanowicz GE, Bigelow EMR, et al. Divergent mechanical properties of older human male femora reveal unique combinations of morphological and compositional traits contributing to low strength. Bone. 2022;163:116481. https://doi.org/10.1016/j.bone.2022.116481.
37. Pfister AK, Welch CA, John M, Emmett MK. Changes in nonosteoporotic bone density and subsequent fractures in women. South Med J. 2016;109:118–123. https://doi.org/10.14423/SMJ.0000000000000410.
38. Whittier DE, Samelson EJ, Hannan MT, et al. Bone microarchitecture phenotypes identified in older adults are associated with different levels of osteoporotic fracture risk. J Bone Miner Res. 2022;37(3):428–439. https://doi.org/10.1002/jbmr.4494.